2020년 2월

박사학위 논문

Improvement of Bone Formation in Calvarial Defected Rat by Modulation of Pore Size in Tricalcium Phosphate Scaffold

조 선 대 학 교 대 학 원

의 학 과

류 강 현

Improvement of Bone Formation in Calvarial Defected Rat by Modulation of Pore Size in Tricalcium Phosphate Scaffold

Tricalcium Phosphate 지지체의 공극 사이즈에 따른 백서 두개골 손상 모델에서 골조직 재생 증진 연구

2020년 2월 25일

조 선 대 학 교 대 학 원

의 학 과

류 강 현

Improvement of Bone Formation in Calvarial Defected Rat by Modulation of Pore Size in Tricalcium Phosphate Scaffold

지도교수 손 홍 문

이 논문을 의학 박사학위신청 논문으로 제출함

2019년 10월

조 선 대 학 교 대 학 원

의 학 과

류 강 현

류강현의 박사학위 논문을 인준함

위원장 조선대학교 교수 이 상 홍 (인)

위 원 조선대학교 교수 이 준 영 (인)

위 원 전남대학교 교수 서 형 연 (인)

위 원 조선대학교 교수 임 원 봉 (인)

위 원 조선대학교 교수 손 홍 문 (인)

2019년 12월

조 선 대 학 교 대 학 원

CONTENTS

LIST OF Tables

LIST OF FIGURES

ABSTRACT

Tricalcium Phosphate 지지체의 공극 사이즈에 따른 백서 두개골 손상 모델에서 골조직 재생 증진 연구

류 강 현

지도교수 : 손 홍 문

조선대학교 대학원 의학과

목적: 골 재건 시 다공성 스캐폴드의 사용은 소실 부위의 골 형성을 촉진시키는 것으로 알려져 있으나 스캐폴드의 공극 크기 및 분포가 골 형성에 미치는 영향에 관한 정확한 기전은 아직 잘 알려져 있지 않다. 따라서 본 연구에서는 백서 두개골 손실 모델에서 다양한 공극 구조를 가진 Beta-TCP 스캐폴드의 이식을 통해 골 형성에 미치는 영향을 분석하였다.

대상 및 방법: 공극 형성 물질로서 매크로 또는 메소 크기의 NaCl 입자를 처리하여 단일 메타 또는 메소 공극의 스캐폴드와 메타와 메소 크기가 혼재하는 스캐폴드를 제조하고, 공극크기를 SEM 을 이용하여 분석하였으며 이를 백서 두개골 손실 모델에 이식하여 4 주후 Micro-CT, H & E 염색 및 면역 조직 화학 분석에 의해 평가를 수행하였다.

결과: 소성 과정에서 두가지 크기 (500-800 μm 및 10-50 μm)의 NaCl 입자로 스캐폴드를 처리하여 Beta-TCP 스캐폴드의 공극 크기와 분포가 제어되는 것으로 관찰되었다. 또한 매크로 및 메소 크기의 다공성 구조가 혼재하는 스캐폴드의

이식이 단일 매크로 및 메소 크기의 다공성 구조보다 Micro-CT 및 조직학적 분석결과 골 형성이 가장 빠르게 촉진되었음을 관찰할 수 있었고, Type-1 Collagen 및 Osteocalcin 단백질 발현의 증가를 유도하였음을 알 수 있었다.

결론: 다양한 크기의 스캐폴드의 기공의 크기는 단일 매크로 및 메소 크기의 다공성 구조보다 생체 내에서 골 형성을 촉진시키는 데 있어서 보다 효과적이며 이를 통한 골 형성 촉진에 있어서 중요한 역할을 하는 것을 알 수 있다.

색인단어: 골 재생, 지지체, Beta-TCP, 공극, 다공성 구조

Ⅰ. INTRODUCTION

Bone graft materials are being increasingly consumed for orthopedic surgeries; world-widely, over 2,000,000 patients are being treated using bone grafts per year.[1,2] Bone grafts are used for accelerating bone formation during the recovering of skeletal fractures or between two bones across a diseased joint, to replace and regenerate lost bone as a result of trauma, infection, or disease, or improve the bone healing response and regeneration of bone tissues around surgical implants.[3] Among the clinically available grafts, autologous bone from patient is still being considered as the gold standard, because of properties required for bone regeneration.[4] However, the limited supply and the associated donor site complications makes concern. The varying nature of available graft determine the resorption ability of these calcium phosphate (CaP)-based graft materials, based on their geometries, porosity, solubility, and densities.[5]

Calcium phosphate is commonly used for orthopedic and dental surgery because of its safety during dissolution and degradation, stability, and desirable porosity and interconnectivity.[6] Moreover, they possess a good adherence to osteoblast cells.[7] Among calcium phosphate ceramics, Beta - tricalcium phosphate (Beta-TCP), which is dissolved by acids released from osteoclasts, is different from hydroxyapatite, which is hard to dissolve. In general, they possess the character of good cell-mediated degradation, which proceeds at the similar time to that of bone formation; this allows formation of new bone with

homogeneous elasticity and makes reduced fracture risk. In recently, a significant progress have been made synthesize the porous.[8,9] Ever since a lot of porous materials have emerged, bone graft with various pore size have been studied.[10] Therefore, the International Union of Physical and Applied Chemistry (IUPAC) has defined various ranges of pore size, i.e., micro-pores (width below 2 nm), meso-pores (width between 2 and 50 nm), and macro-pores (width above 50 nm), which will be investigated throughout present research.[11] Macro-pores with diameters greater than 50 nm are usually needed to improve the adhesion of osteoblasts for enhancing the osteo-induction ability of the scaffolds.[10,12] Interconnected micro- and meso-pores leads to promote body-fluid circulation and cellular migration to the the implant.[13] Although the detail mechanisms by which the macro-pores s improve the osteogenic functions of cells and bone formation are still unclear, the hypotheses can be explained in previous researches.[10] If the pore is too small, cell cannot migrate into the center of construct, thus limited diffusion of nutrients and removal of waste products. In contrast, the pores are too large, they decreases the specific surface available, thereby limiting attachment.[14] Thus, producing ceramic in which the width of the macro- and meso-pores could be controllable to make an unmet medical use; these will provide more surface for cell attachment and differentiation. But, these ceramics have relatively complicated process for manufacturing; alternatively, the size of their macro- and meso-pores and their porosities cannot be controlled well. In previous study, hierarchically ordered macro-porous calcium phosphate scaffold have

been fabricated the cement in presence of sodium chloride (NaCl) debris utilizing the leaching process.[10] In this process, NaCl particles (used as the name of porogen) of multipe sizes have been used for producing macro-pores s or meso-pores within scaffolds. The research showed that high interconnected meso-pores with 2-50 μm width were distributed across the macro-pores, and the shape of each pore was very irregular.[15] Therefore, scaffold designing strategies have to be able to create hierarchical ordered pore structures to simultaneously attains optimal mass transport properties, mechanical stiffness, and cell-tissue colonization and infiltration within the whole scaffold microarchitecture.

In this study, a molten salt manufacturing process was used to prepare multi-pore sized Beta-TCP, and their constituent macro- (width ranging from 200 to 800 μm) and meso-pores (2 to 50μm), porosities, and the performances were analyzed and compared to those of ceramics comprising pores of only a single size in calvarial defected rat model. The bone formation was analyzed by the radiological and histological evaluation, in which Beta-TCP scaffolds that comprised pores with different sizes and had controlled architectures were implanted.

II. MATERIALS AND METHODS

1. Beta-TCP scaffolds

The Beta-TCP block forms were manufactured in SN Global Company (Gwang-Ju, Korea). The Beta-TCP powders were weighed to ratio percentage of 20 to 40. Sodium chloride (NaCl) particles were weil-ground and sieved; and then they were then separated based on the indicated diameters (Table 1). Sodium chloride particles of each size (macro- or meso-particles) were added into the mixed Beta-TCP powders, followed by mixing in a 3D blender (a; treatment with NaCl porogen particles that were 200-300 μm in size, b; treatment with NaCl porogen particles that were 200-300 μm and 10-50 μm in size, respectevely, c; treatment with NaCl porogen particles that were 500-800 μm in size, d; treatment with NaCl porogen particles that were 500-800 μm and 10-50 μm in size, respectevely). The mixed powders were molded and compacted and then the mixtures were heated to 800° C, allowed to stand for 1hr, and then cooled in air. Finally, the Beta-TCP block including NaCl porogen removed from its mold, immersed on distilled water (DW), and then dried. The scaffolds are shown in Fig. 1.

2. Structural analysis of the Beta-TCP blocks

The pore size of manufactured Beta-TCP blocks were observed and analyzed by scanning electron microscopy (SEM; Hitachi S-4800, Tokyo, Japan) to determine the macro- and meso-pore sizes, according to a previous protocol[10]. The average pore size was calculated from the pictures.

3. Animals

A total of 48 male specific-pathogen-free Wistar rats aged 10 weeks and weighing 200-250 g were provided from Orient Bio Co. (Gwang-Ju, Korea). The animal research ethics committee of the Chosun University approved the study (CIACUC2016-S0001). The animals were housed on sawdust bedding and received food pellets and water ad libitum. All behavioral experiments were performed during the light phase of the cycle, i.e. The rats were acclimatized to environment for 1 week before experiment.

4. Surgical calvaria defects

To make the calvaria defect model, the surgical procedures were carried out according to previous study.[16] The rats were anesthetized by intraperitoneal (IP) injection of pentobarbital sodium (Sigma-Aldrich, St. Louis, MO) at 30 mg/kg. Subsequently, 20mm linear incisions were created on the dorsal part on the cranium and periosteums were removed. A bony defect was created to full thickness of 6mm in the parietal bone (Fig. 2). PBS was irrigated into the injury site for cooling, and the dura mater was kept intact during the procedure. After the defect were implanted with the indicated Beta-TCP blocks, the skin was closed. After 4 weeks, the animals were sacrificed and the samples were acquired.

5. Micro-computed tomography (micro-CT)

The skull was dissected from the mouse in each group and micro-CT imaging was acquired from a Quantum GX micro-CT imaging system (PerkinElmer, Hopkinton, MA, USA) at the Korea Basic Science Institute in Gwangju, Korea. The X-ray source was set at 90 kV and 88 mA, with a field of view of 45 mm (voxel size, 90 μm; scanning time, 14 min). CT images were viewed using the Quantum GX 3D Viewer software.

6. Histologic evaluation

The mouse skull was fixed in 10% formalin (pH 7.4) for 48 h at 37° C. Bone tissues were first decalcified using sodium citrate solution before they were processed and mounted onto the histological slides. Decalcified skulls were cut at the midpoint and embedded in paraffin blocks. Serial paraffin sections were stained with hematoxylin and eosin (H&E). Images of the stained tissues were captured using a microscope slide scanner (3D-HISTECH Ltd., Budapest, Hungary).

7. Immunohistochemical analysis

Tissue sections (3μm thick sections) were de-paraffinized by soaking in xylene solution and rehydrated using a graded series of ethanol/distilled water solutions. For antigen retrieval, the slides were placed in 0.01 M citrate-buffer (pH 6.0) and heated in a steamer for 30 min. Endogenous peroxidases were stained by incubation with 3% hydrogen peroxide for 20 min

at room temperature. The sections were incubated 24hrs at 4° C with the following primary antibodies (1:50 dilution): anti-type 1 collagen (Santa-Cruz Biotechnology, Santa-Cruz, CA, USA) and anti-osteocalcin (Santa-Cruz Biotechnology). Subsequently, the sections were incubated with a biotinylated secondary antibody (LSAB; Dako Cytomation, Glostrup, Denmark, K0675) for 30 min, washed in PBS, and incubated with a streptavidin-peroxidase conjugate (LSAB, Dako Cytomation, K0609) for 30 min. The reaction was performed using 3,3'-diaminobenzidine tetrahydrochloride (Sigma-Aldrich, S-1141) for 5 min. The slides were briefly counterstained in hematoxylin and dehydrated; a cover slip was then placed on each slide. Negative and positive controls were run simultaneously. Mammary tissues served as the positive control. Images were captured using a microscope slide scanner (3D-HISTECH Ltd).

8. Statistical analysis

All experiments were performed in triplicate. Data were expressed as the means ± SDs and analyzed using analysis of variance (ANOVA) using SPSS for Windows (version 12.0; SPSS, Chicago, IL, USA) to determine significant differences. The threshold of statistical significance was set at $p < 0.05$.

III. RESULTS

1. Observation of the Beta-TCP blocks structures

According to the SEM analysis, the Beta-TCP blocks were observed to have a wider range of macro-pores diameters over 200 μm (Fig. 3). The average macro-pore sizes of scaffolds a, b, c, and d were measured to approximately 380 μm, 565 μm, 598 μm and 572 μm, respectively. The macro-pores of scaffolds a and c were more uniformed than those of scaffolds b and d. Furthermore, the macro-pores of scaffolds b and d showed wider diameter than that of a and c.

In addition, a lot of interconnecting meso-pores were observed in scaffold d (Fig. 4). However, these interconnected meso-pores could not be observed in scaffold b although porogen particles with a size of 10-50 μm (meso-sized particles) were treated during manufacturing process.

2. Radiological analysis of the Beta-TCP blocks

The bony recover effects by the treatment of different scaffolds were analyzed by micro-CT observation, as it can provide abundant and powerful information. 3D rendering reconstructions of the defects implanted with the different scaffolds by micro-CT are shown in Fig. 5. Overall, implantation of the Beta-TCP scaffolds led a desirable bone recover in the rats with calvarial bone defects.

3. Histopathological findings

As indicated in Fig. 6, the bone formation were monitored in the scaffolds b and d implanted at the rat calvarial defect sites. Especially, scaffold d into the calvarial defects resulted in significant osteogenesis at the bone lesion site. One specimen showed the presence of newly formed bone not only at an area adjacent to the bone cortex, but also inside the pores of scaffold d. In addition, implanted materials were observed in case of the implantation of the scaffolds a, b, and c, while no notable implanted materials were seen in case of scaffold d.

These results of the animal study suggest that scaffold d, which had a controlled, multi-pore sized structure, resulted in a satisfactory amount of osteogenesis and bioresorption in the early stage after its implantation into the site of calvarial defects.

4. Immunohistochemical study of collagen type 1 and osteocalcin expressions

As a new bone formation should be accompanied by the expression of specific proteins that mark osteogenic progression, the sections of the bone defects were subjected to qualitative immunohistochemical studies. The host bone and regions which is adjacent to the defect sites demonstrate that type I collagen, an early specific marker of osteoblastic proliferation, had a significantly high intensity in the scaffold d-implanted bone defect sites (Fig. 7A).

In addition, expressions of osteocalcin, a late marker of osteoblastic

differentiation and mineralization, increased in case of the implantation of all the scaffolds (Fig. 7B). Notably, the newly formed bone integrated well with the edge of the host bone and scaffold struts, and the osteocalcin expression was high in case of the implantation of not only scaffold d, but also the other scaffolds.

IV. Discussion

Tissue scaffolds are one of the most optimal choices to repair bone defects. The scaffold should be designed to mimic the bone morphology, for optimizing their integration into the surrounding tissues.[17] The macro-pores are necessary for new bone formation because they allow the migration and proliferation of pre-osteoblasts, as well as vascularization.[18] The macro-pores required to regenerate mineralized bone is considered to be 100-800㎛; however, such scaffolds could have poor mechanical strengths.[19] For these reasons, multi-pore sized scaffolds have been announced to increase the mechanical strength and biological properties of scaffolds, and several studies have reported that multi-pore sized scaffolds comprising micro- and macro-pores perform better than scaffolds comprising only macro-pores.[20] Uniform macro-pores and many interconnecting pores have been reported to be essential for bone tissue penetration, and these structures have been reported to increase the compressive strength of the scaffold, compared to the case for other scaffolds with the same composition and porosity.[21] Especially, the average pore diameter in case of scaffold d was under 100㎛, which is significantly lower than the case for other scaffolds. Therefore, treatment of the scaffolds with sodium chloride particles that were 500-800 ㎛ diameter, along with those that were 10-50 ㎛ led to the synthesis of multi-pore sized scaffolds comprising macro-pores and many interconnecting pores.

Also, b and d scaffolds showed a good adhesion properties with the margin of

the defective bone, compared to the case for scaffolds a and c. This indicates that additional treatment of the scaffold with meso-sized porogen particles led to an improved adhesion between the interconnected meso-pores of the scaffold and pre-osteoblast cells. In a scaffold in which the meso-pores are not fully interconnected, bone ingrowth should generally be faster when larger macro-pores s are present. Scaffolds used for promoting osteogenesis should mimic the morphology, structure, and function of bone for their optimal integration into the surrounding tissue. According to a study by Baumgart and Bohner, bone ingrowth is affected by the pore diameter as long as the structure is fully interconnected and the pore interconnections have a diameter larger than 50㎛.[22] Since perfect bone repair is the ultimate goal of the scaffolds used for bone tissue engineering, the bone repair effects of the Beta-TCP scaffolds were carefully evaluated. To further obtain an insight into the bone repair effects of various scaffolds, histological sections of the bone defects were analyzed by micro-CT imaging.[23] Moreover, changes of new bone formation induced by the different scaffolds were synchronized with the micro-CT images.[24]

Type I collagen is considered to an early proliferation marker of osteoblasts; it means that the pre-osteoblasts showed high proliferation following the implantation of scaffolds comprising multiple-sized pores.[25] This indicates that the multi-pore sized structure of scaffold d was suitable for the penetration of newly formed bone tissue into the pores of the scaffold at a early stage.

V. Conclusion

The multi-pore sized scaffold exhibited a greater macro- and mesopore diameter, achieved better bone repair at the early stage of injury. In contrast, the Beta-TCP scaffold with a small macro-pores and no meso-pores displayed a greater potential for the long-term repair of bone defects, as Beta-TCP possesses a higher *in vivo* absorbability, which was strongly evidenced by the micro-CT reconstructions and histological examinations. Since the variables of the multi-pore sized scaffolds were controlled based on the pore size, which can be achieved by the simple treatment of Beta-TCP with porogen particles of variable sizes for bone defect repair. These results provide important insights into the synthesis of scaffolds with optimal efficiency for bone tissue engineering and, it was proposed that osteogenic proliferation and differentiation *in vivo* was enhanced by the presence of multiple-sized pores.

REFERENCES

1. Wang W, Yeung KWK. Bone grafts and biomaterials substitutes for bone defect repair: A review. Bioact Mater. 2017;2:224-47.

2. Campana V, Milano G, Pagano E, et al. Bone substitutes in orthopaedic surgery: from basic science to clinical practice. J Mater Sci Mater Med. 2014;25:2445-61.

3. Polo-Corrales L, Latorre-Esteves M, Ramirez-Vick JE. Scaffold design for bone regeneration. J Nanosci Nanotechnol. 2014;14:15-56.

4. Bauer TW, Muschler GF. Bone graft materials. An overview of the basic science. Clin Orthop Relat Res. 2000:10-27.

5. Sheikh Z, Najeeb S, Khurshid Z, Verma V, Rashid H, Glogauer M. Biodegradable Materials for Bone Repair and Tissue Engineering Applications. Materials (Basel). 2015;8:5744-94.

6. Kasten P, Beyen I, Niemeyer P, Luginbuhl R, Bohner M, Richter W. Porosity and pore size of beta-tricalcium phosphate scaffold can influence protein production and osteogenic differentiation of human mesenchymal stem cells: an in vitro and in vivo study. Acta Biomater. 2008;4:1904-15.

7. Kasten P, Luginbuhl R, van Griensven M, et al. Comparison of human bone marrow stromal cells seeded on calcium-deficient hydroxyapatite, beta-tricalcium phosphate and demineralized bone matrix. Biomaterials. 2003;24:2593-603.

8. Li X, van Blitterswijk CA, Feng Q, Cui F, Watari F. The effect of calcium

phosphate microstructure on bone-related cells in vitro. Biomaterials. 2008;29:3306-16.

9. Li X, Liu H, Niu X, et al. Osteogenic differentiation of human adipose-derived stem cells induced by osteoinductive calcium phosphate ceramics. J Biomed Mater Res B Appl Biomater. 2011;97:10-9.

10. Zhang K, Fan Y, Dunne N, Li X. Effect of microporosity on scaffolds for bone tissue engineering. Regen Biomater. 2018;5:115-24.

11. Soler-Illia GJ, Sanchez C, Lebeau B, Patarin J. Chemical strategies to design textured materials: from microporous and mesoporous oxides to nanonetworks and hierarchical structures. Chem Rev. 2002;102:4093-138.

12. Murphy CM, Haugh MG, O'Brien FJ. The effect of mean pore size on cell attachment, proliferation and migration in collagen-glycosaminoglycan scaffolds for bone tissue engineering. Biomaterials. 2010;31:461-6.

13. Reinwald Y, Johal R, Ghaemmaghami A, Rose F, Howdle S, Shakesheff K. Interconnectivity and permeability of supercritical fluid-foamed scaffolds and the effect of their structural properties on cell distribution. Polymer. 2014;55:435-44.

14. Murphy CM, O'Brien FJ. Understanding the effect of mean pore size on cell activity in collagen-glycosaminoglycan scaffolds. Cell Adh Migr. 2010;4:377-81.

15. Wei J, Jia J, Wu F, et al. Hierarchically microporous/macroporous scaffold of magnesium-calcium phosphate for bone tissue regeneration. Biomaterials. 2010;31:1260-9.

16. Diao J, OuYang J, Deng T, et al. 3D-Plotted Beta-Tricalcium Phosphate Scaffolds with Smaller Pore Sizes Improve In Vivo Bone Regeneration and Biomechanical Properties in a Critical-Sized Calvarial Defect Rat Model. Adv Healthc Mater. 2018;7:e1800441.

17. Dai W, Kawazoe N, Lin X, Dong J, Chen G. The influence of structural design of PLGA/collagen hybrid scaffolds in cartilage tissue engineering. Biomaterials. 2010;31:2141-52.

18. Bose S, Roy M, Bandyopadhyay A. Recent advances in bone tissue engineering scaffolds. Trends Biotechnol. 2012;30:546-54.

19. Karageorgiou V, Kaplan D. Porosity of 3D biomaterial scaffolds and osteogenesis. Biomaterials. 2005;26:5474-91.

20. Woodard JR, Hilldore AJ, Lan SK, et al. The mechanical properties and osteoconductivity of hydroxyapatite bone scaffolds with multi-scale porosity. Biomaterials. 2007;28:45-54.

21. Sopyan I, Fadli A, Mel M. Porous alumina-hydroxyapatite composites through protein foaming-consolidation method. J Mech Behav Biomed Mater. 2012;8:86-98.

22. Bohner M, van Lenthe GH, Grunenfelder S, Hirsiger W, Evison R, Muller R. Synthesis and characterization of porous beta-tricalcium phosphate blocks. Biomaterials. 2005;26:6099-105.

23. Guda T, Darr A, Silliman DT, et al. Methods to analyze bone regenerative response to different rhBMP-2 doses in rabbit craniofacial defects. Tissue Eng Part C Methods. 2014;20:749-60.

24. Sawyer AA, Song SJ, Susanto E, et al. The stimulation of healing within a rat calvarial defect by mPCL-TCP/collagen scaffolds loaded with rhBMP-2. Biomaterials. 2009;30:2479-88.

25. Sun L, Pereira D, Wang Q, et al. Controlling Growth and Osteogenic Differentiation of Osteoblasts on Microgrooved Polystyrene Surfaces. PLoS One. 2016;11:e0161466.

Table 1. Diameter range of the porogen particles used for treating the scaffolds A, B, C, and D

Scaffold	A	B	C	D
Porosity (%)	65	65	65	65
Diameter range of Macro-sized particles (μm)	200-300	200-300	500-800	500-800
Diameter range of Meso-sized particles (μm)	-	10-50	-	10-50
Weight ratio of porogen (%)	60	80	60	80

Figure 1. The Beta-TCP block of the scaffolds a, b, c, and d. The visible pores were observed in case of all the scaffolds. The surface of each scaffold is irregular in shape, and for the implantation into the rat calvarial defect site, each scaffold was cut and fit into the defect site.

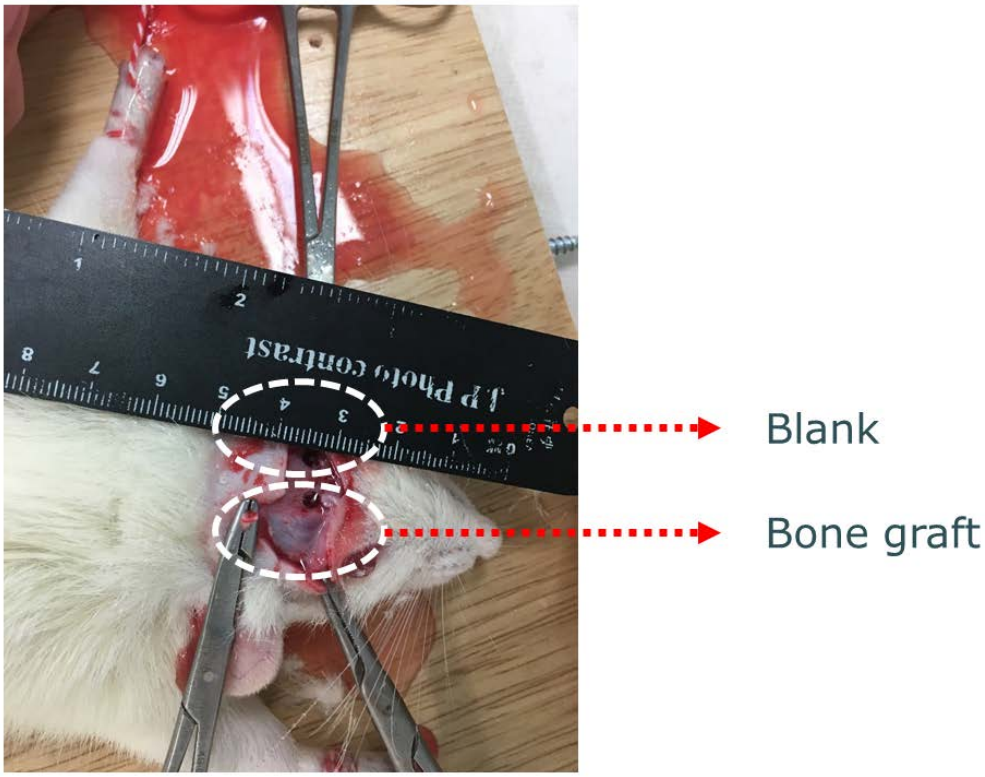

Figure 2. Surgical creation of calvarial defects and bone graft implantation.

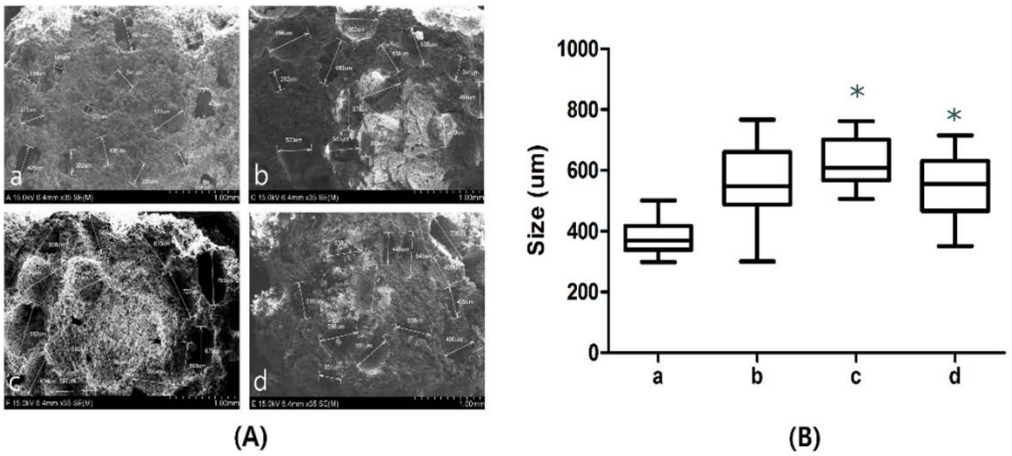

Figure 3. SEM pictures of the scaffolds a, b, c, and d at 35× magnification, showing the macro-pores diameter of the scaffolds. All macro-pores s were monitored by SEM (A). The macro-pores diameters were measured and the data in the bar graphs are expressed as the means ± standard deviations (SDs). The significant differences were *P<0.05 with other groups (B).

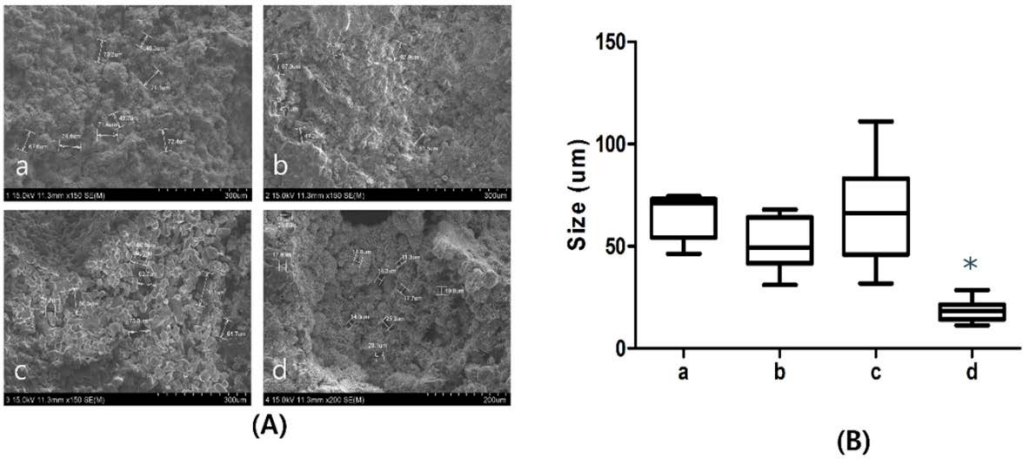

Figure 4. SEM pictures of the scaffolds a, b, c, and d at 200× magnification, showing the mesopore diameter (<100 μm, >2 μm) of the scaffolds. All meso-pores were monitored by SEM (A). The macro-pores diameters were measured and the data in the bar graphs are expressed as the means ± standard deviations (SDs). The significant differences were *P<0.05 with other groups (B).

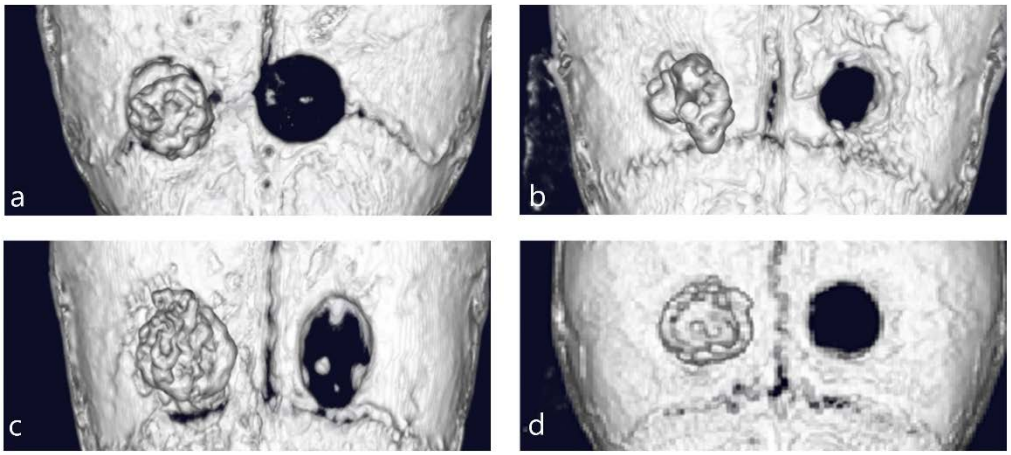

Figure 5. Micro-CT assessments of the repaired bone defects. Micro-CT reconstructions of the calvarial defects in rats repaired using the scaffolds a, b, c and d at 4 weeks after implantation. The right side of the calvarial defects (with no implantation) served as the blank control.

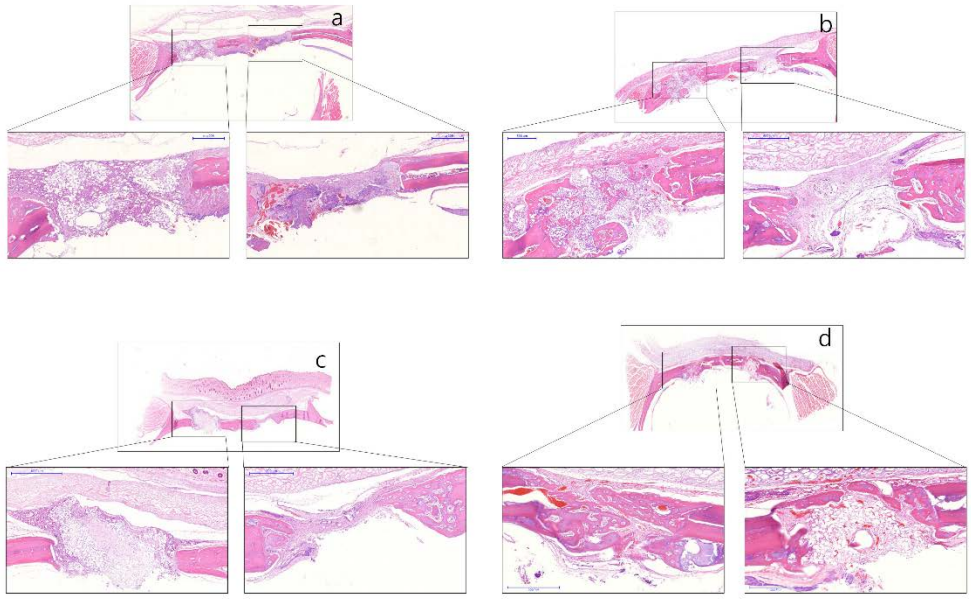

Figure 6. Histological examination of the calvarial defects in rats repaired using the scaffolds a, b, c and d at 4 weeks after implantation. The right side of the calvarial defects (with no implantations) served as the blank control. The upper pictures were obtained at 20× magnification, and the lower pictures, at 100× magnification.

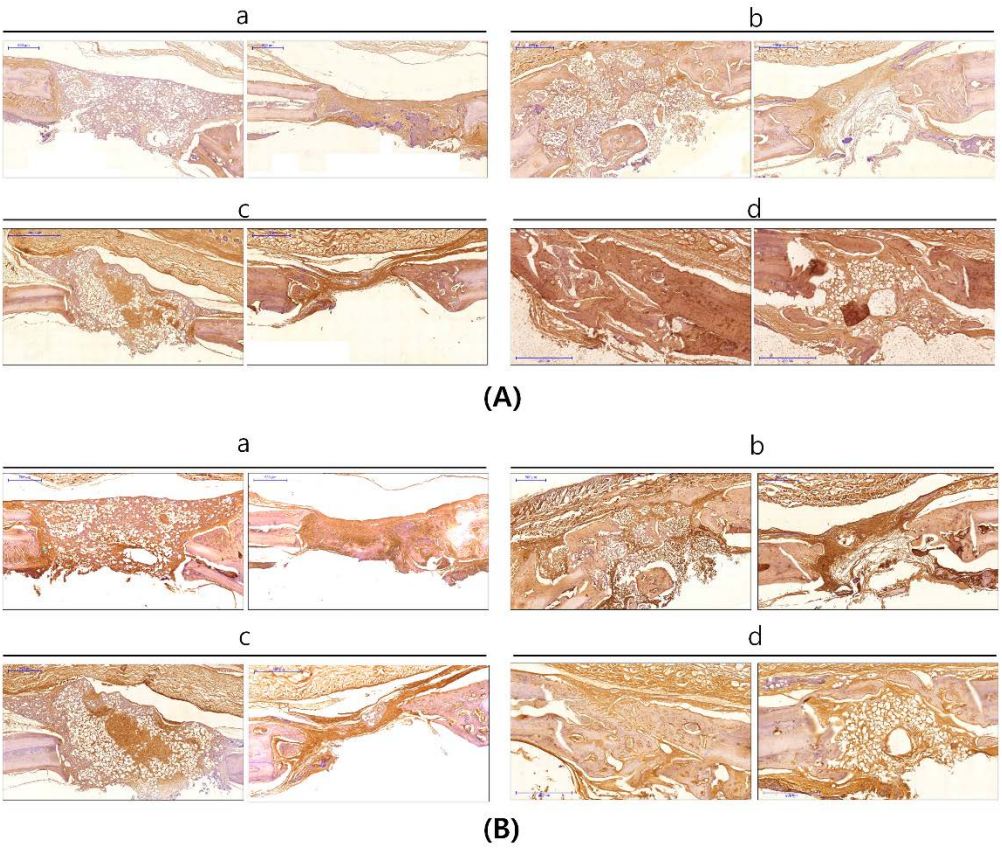

Figure 7. Immunohistochemical study of the calvarial defects in rats implanted with the scaffolds a, b, c and d at 4 weeks after implantation. The type 1 collagen (A) and osteocalcin (B) protein expression was observed at 100× magnification. The right side of the calvarial defects (with no implantation) served as the blank control.